**HGGA, Volume *3***

## Supplemental information

# Stx4 is required to regulate cardiomyocyte $Ca^{2+}$ handling during vertebrate cardiac development

**Eliyahu Perl, Padmapriyadarshini Ravisankar, Manu E. Beerens, Lejla Mulahasanovic, Kelly Smallwood, Marion Bermúdez Sasso, Carina Wenzel, Thomas D. Ryan, Matej Komár, Kevin E. Bove, Calum A. MacRae, K. Nicole Weaver, Carlos E. Prada, and Joshua S. Waxman**

**Supplemental Information**

**Table of Contents** **page**

**Supplemental note: Case Report for Patient 1**

Patient 1 presented with progressive fatigue at three years of age. Initial evaluation in the emergency room was significant for increased work of breathing, hypotension, and severe acidosis. Previous medical history was significant for congenital profound sensorineural hearing loss, hypotonia, and global developmental delays. Echocardiography showed Patient 1 to have dilated cardiomyopathy (DCM) with severely depressed biventricular systolic function, and he was electively intubated and managed with calcium and milrinone infusion to augment cardiac output. Patient 1 developed frequent ectopy (premature atrial and ventricular contractions) with runs of non-sustained ventricular tachycardia (VT). Subsequently, he was placed on extracorporeal membrane oxygenation (ECMO) and continued to have hypotension and episodes of VT. Patient 1 was initially managed with propranolol but required an esmolol drip due to the progressive arrhythmia. Due to his instability, a transeptal puncture with bladed and serial balloon atrial septoplasty was performed and resulted in substantial left atrial decompression with overall improvement of right atrial and ventricular filling and systolic function. Patient 1 was subsequently placed on a Berlin Heart EXCOR® left ventricular assist device (LVAD) and continued to have prolonged episodes of VT, requiring amiodarone and atrial single chamber (AAI) pacing for a period of time. The LVAD was changed to a CentriMag™ Extracorporeal Blood Pumping System to better unload the left ventricle. He was then placed on a biventricular assist device (BiVAD), which improved LVAD filling and cardiac output but did not affect his continuous VT. Ultimately, Patient 1 received an orthotopic heart transplant (OHT) two months from the onset of his initial symptoms. Patient 1's muscular weakness was progressive after OHT, and he required a tracheostomy with ventilatory support for the inability to tolerate coming off of mechanical ventilation. His course since transplant has been notable for multiple infections, likely related to chronic immunosuppression, as well as poor somatic growth on enteral feeds. He remains ventilator dependent. The transplanted heart shows normal function without evidence for graft coronary artery disease at five years of age, and there have been no significant episodes of rejection. Despite atrial tachycardia shortly after transplant, he has been weaned off beta blocker therapy and has had no further ectopy, to date. Patient 1 is nine years of age at the time of publication and has

a sibling who is regularly screened for DCM and is asymptomatic as of five years of age. The sibling is homozygous for the reference (WT) *STX4* allele (Figure S2).

**Supplemental note: Case Report for Patient 2**

Patient 2 presented upon fetal ultrasound at 25+0 weeks of gestation with multiple anomalies including frontal edema, persistent ductus arteriosus, oligohydramnios, hypoplastic kidneys, severely dilated echogenic small bowel loops, duodenal atresia, and overlapping fingers. At 30+4 weeks of pregnancy, Patient 2 was delivered via secondary cesarean section due to complications of anhydramnios and induction of premature labor. TORCH complex was excluded prenatally, and there were no signs of other noxious agents during pregnancy. At delivery, Patient 2 exhibited normal birth measurements including, size, weight, and head circumference; however, a short umbilical cord was noted. Upon postnatal evaluation, Patient 2 exhibited multiple malformations, including pulmonary hypoplasia, hepatomegaly, duodenal atresia, renal dysplasia, a small urinary bladder, scoliosis, clubfoot, and musculoskeletal contractures of the right hand, elbow, and foot (Figure S3). Postnatal echocardiography showed normal heart arrangement, a patent foramen ovale with aneurysms of the septum, a persistent ductus arteriosus, and T1 1-2° and moderately reduced left ventricular-function. The patient also displayed facial dysmorphia, including retrognathia, a tent-shaped mouth and small, dysplastic low-set, posteriorly rotated ears. Due to the prenatal WES, chromosomal analysis was performed after birth but was normal. In addition to the multiple congenital anomalies, Patient 2 had massive ubiquitous edema and required ventilatory support; he subsequently died five days after birth. Upon autopsy, the cause of death was determined to be consistent with multi-organ failure. A cerebral MRI performed post-mortem indicated a subarachnoid hemorrhage, but was unremarkable for neuronal migration or gyration disorders, although partial pachygyria was noted upon autopsy. Other pertinent findings included renal hypoplasia, pulmonary hypoplasia, and malposition of the vermiform appendixis. Calcifications on the posterior wall of the heart were also noted; the patent foramen ovale and persistent ductus arteriosus were documented to be consistent with the early gestational birth. Aspects of the pleotropic phenotypes listed were differentially noted to possibly be secondary to the anhydramnios/oligohydramnios or due to gestational

age at delivery. However, the etiology of the anhydramnios was not clinically resolved. Patient 2 has one sibling who is healthy as of four months of age. Notably, the mother's first pregnancy terminated as a spontaneous abortion in the first trimester. Genetic testing of the living sibling was unavailable at time of publication (Figure 1C).

## Supplemental Figures

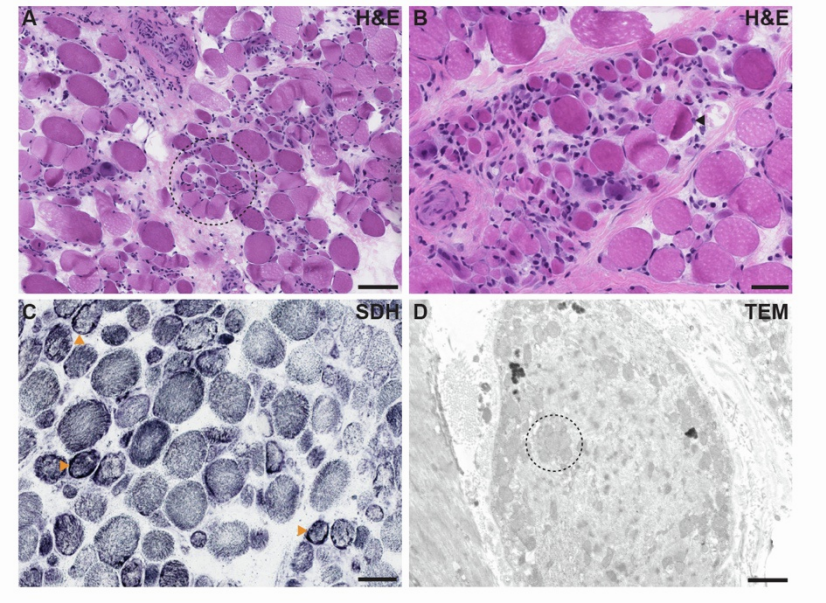


**Figure S1. Histopathology of heart and skeletal muscle biopsy of Patient 1.** (A,B) Cross-sections from a biopsy of the explanted heart of Patient 1 stained with hematoxylin-eosin. (A) Diminished myocardial cross-striations, interstitial fibrosis, hypertrophic fibers, loss of myofibrillar volume, and marked variation in fiber size (circled) are observed. Scale bar: 100 μM. (B) Micrograph of the explanted heart at high magnification shows numerous mainly rounded atrophic fibers (arrowhead), both single and in small groups. Scale bar: 50 μM. (C) Succinic acid dehydrogenase staining of skeletal muscle biopsy shows a normal quantity and distribution of mitochondria in most fibers and the occasional ragged blue fiber (orange arrowheads). Scale bar: 50 μM. (D) Transmission electron micrographs of skeletal muscle biopsy show endomysial fibrosis, increased mitochondrial aggregates (circled), with multiple scattered fibers showing regeneration or degeneration. No significant inflammatory infiltrates are detectable, nor is there appreciable vacuolization within the myofibers. Scale bar: 2 μM.

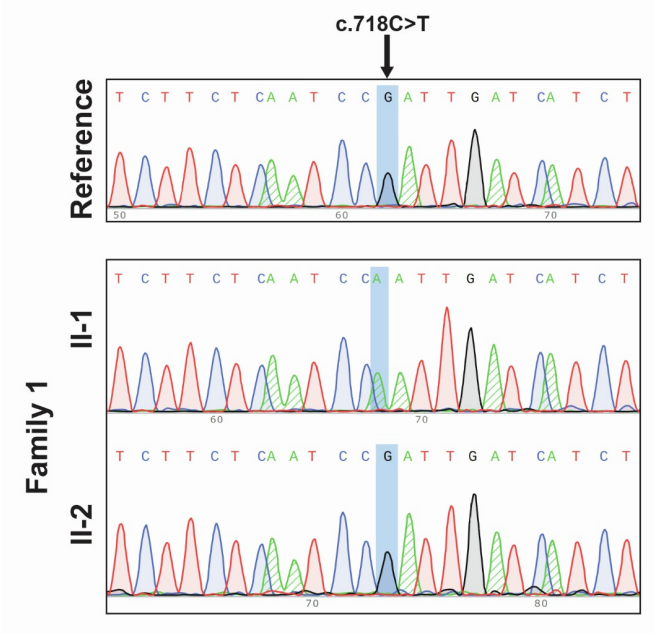


**Figure S2. Targeted *STX4* variant testing of Patient 1 and sibling.** Chromatogram traces of the amplified complementary *STX4* sequence in both Patient 1 (II-1) and their sibling (II-2) compared to an unaffected control individual (reference). Arrow indicates the position of the c.718C>T variant. Patient 1 is homozygous for the variant, while their sibling is homozygous for the reference allele as compared to the unaffected individual.

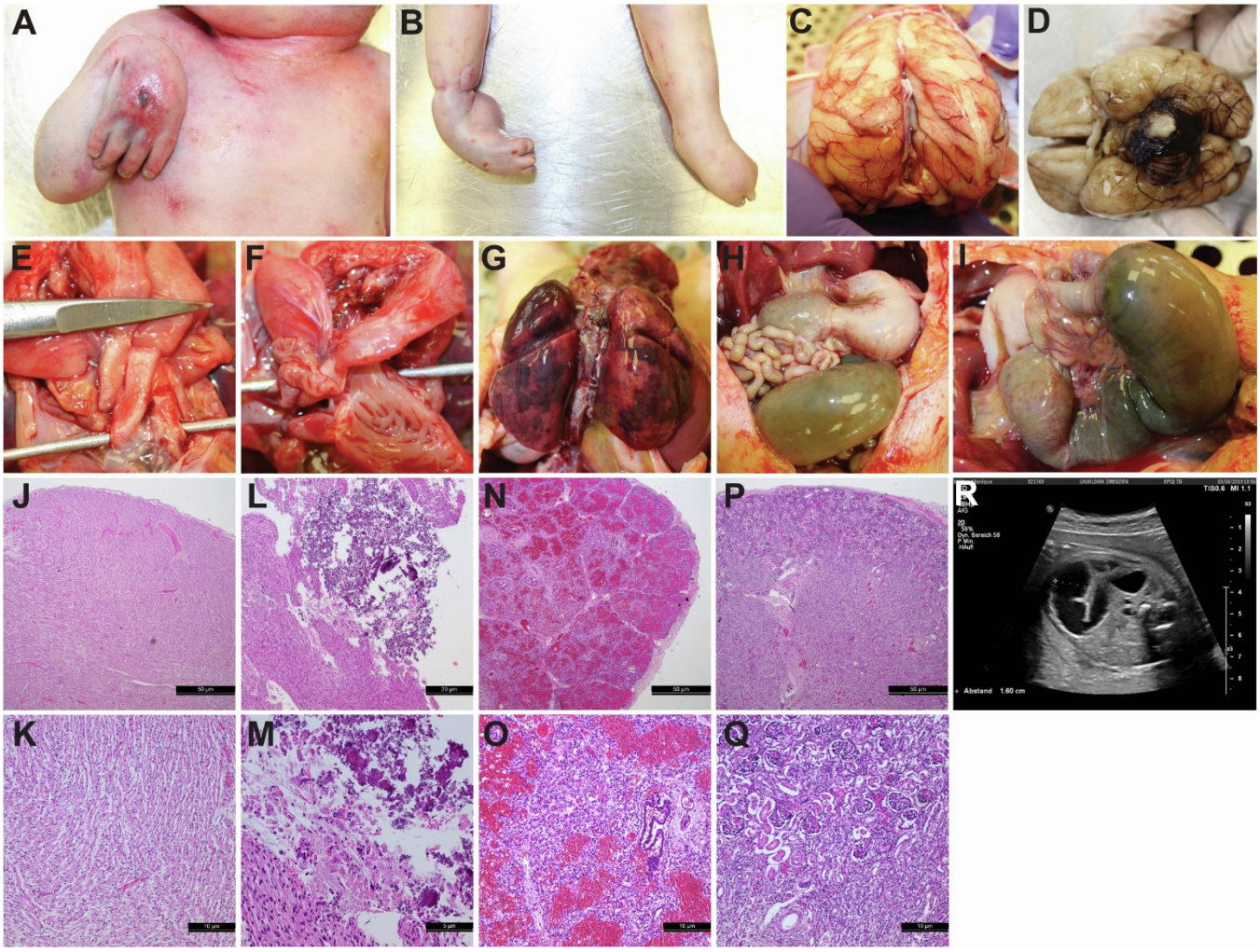


**Figure S3. Autopsy and gross histology of patient with compound heterozygous truncating *STX4* variants.** (A,B) External malformations of patient 2 depicting hyperflexion of the right hand and clubfoot, respectively. (C,D) Pachygyria of the cerebral cortex and cerebellar subarachnoid hemorrhage, identified upon autopsy. (E,F). Persistent ductus arteriosus (PDA) and patent foramen ovale, respectively, are noted with probes demarcating each defect. (G) Lung lobes depicting grossly normal appearance. (H,I) Stenotic ileum with prestenotic dilatation of the duodenum/ileum as well as stomach. (J-M) Cross-sections from a biopsy of the explanted heart of Patient 2 stained with hematoxylin-eosin. (J) Anterior wall of the heart is grossly normal (Scale bar: 50 μM), and (K) without significant signs of hypertrophy (Scale bar: 10 μM). (L,M) Dystrophic calcification was observed on the posterior wall of the heart, without significant signs of hypertrophy. Scale bars: 20 μM and 5 μM, respectively. (N,O) Cross-sections from lung shows partially developed, somewhat delayed lung parenchyma. Scale bars: 50 μM and 10 μM, respectively. (O) Parenchyma at saccular stage of development with acute blood congestion. (P,Q) Cross-sections from kidney show slightly hypoplastic kidneys with regularly developed kidney parenchyma. 50 μM and 10 μM, respectively (R) Prenatal ultrasound of patient 2 depicts abnormal, severely dilated intestinal loop.

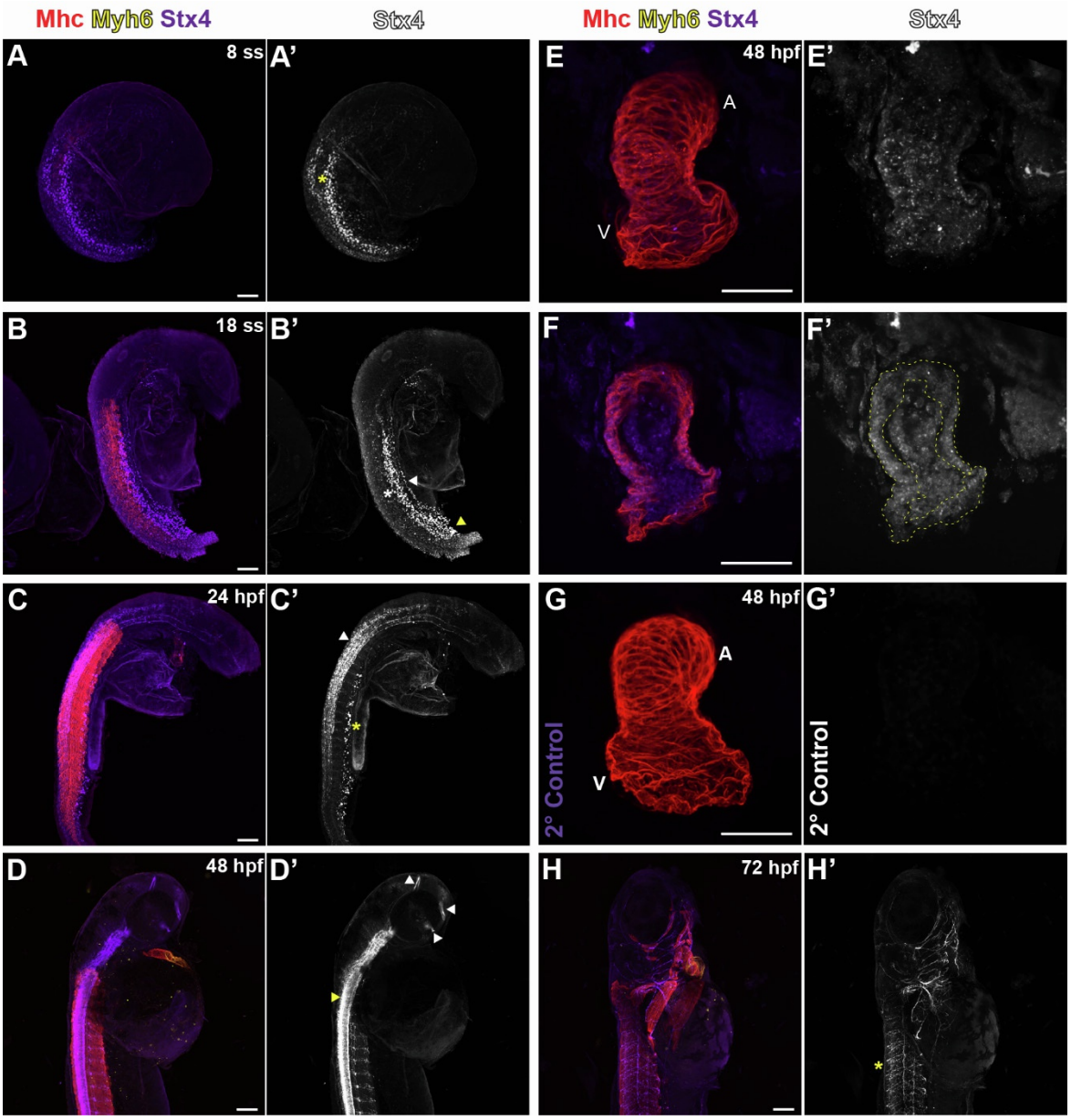


**Figure S4. Stx4 expression is temporally refined during zebrafish development.** (A-H') Confocal max intensity projections (MIPs) of embryos at the 8-somite stage (ss), 18 ss, 24 hpf, 48 hpf, and 72 hpf. IHC for Mhc (striated muscle - red), Myh6 (atrial cardiomyocytes (CMs) - yellow), and Stx4 (purple). (A'-H') Single channel micrographs of Stx4 in A-H. (A,A') At the 8 ss, Stx4 is enriched in the posterior lateral mesoderm (yellow asterisk). (B,B') At the 18 ss, Stx4 becomes refined to the ventral vasculature (white arrowhead), blood progenitors (yellow arrowhead), and pronephros (white asterisk). (C,C') At 24 hpf, Stx4 is enriched in ventral vascular cells (asterisk) and spinal cord (white arrowhead). (D,D') By 48 hpf, Stx4 becomes predominantly neuronally-enriched in several forebrain white matter tracts (including the habenula, posterior, and post-optic commissures (white arrowheads), and spinal cord (yellow arrowhead)). (E,E') Confocal image of Stx4 expressed in the heart at 48 hpf (white puncta). (F,F') MIP of a partial Z-stack of the heart shown in E. Stx4 signal intensity was enhanced relative to E,G and E',G', respectively, to show clear demarcation of Stx4 expression in the heart, including in the myocardium (outlined). (G,G') 48 hpf zebrafish heart stained for Mhc (red) and secondary antibody used for Stx4 antibody alone (anti-rabbit IgG(H+L) Alexa Fluor®-647) (negative control) demonstrates the specificity of the Stx4 antibody staining in the heart at 48 hpf. A: atrium; V:

ventricle. (H,H') At 72 hpf, Stx4 is expressed predominantly in the peripheral nervous system (yellow asterisk indicates motor neurons in the axial myomeres). (A-D,H) Scale bar: 100 μM. (E-G) Scale bars: 50 μM.

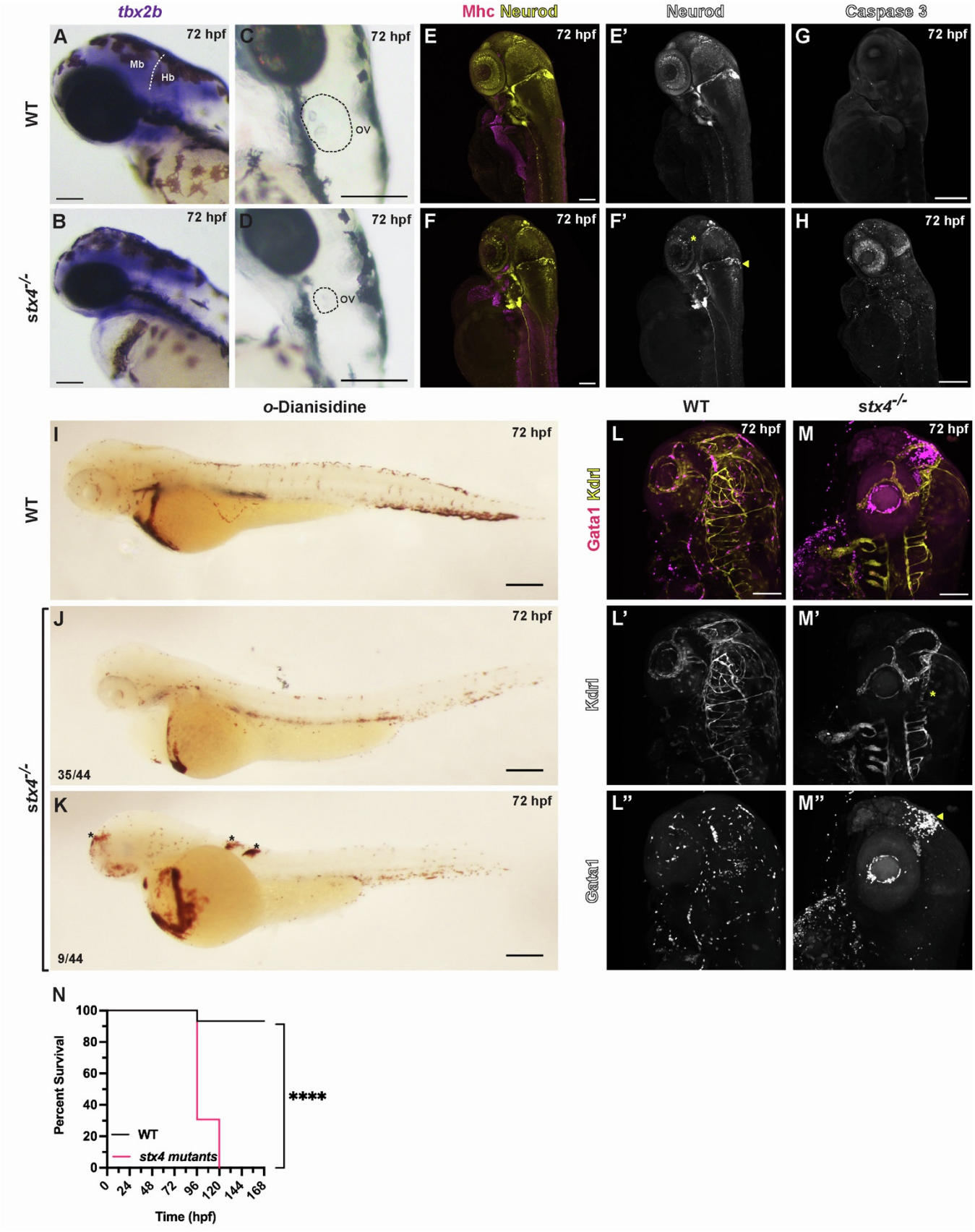
tbx2b
Mhc Neurod
Neurod
Caspase 3
WT
stx4-/-
A
B
C
D
E
E'
F
F'
G
H
72 hpf
Mb
Hb
ov
o-Dianisidine
WT
stx4-/-
I
J
K
35/44
9/44
L
M
L'
M'
L''
M''
Gata1 Kdrl
Kdrl
Gata1
N
Percent Survival
Time (hpf)
WT
stx4 mutants
****

**Figure S5. Stx4 is required for neurodevelopment and vasculogenesis.** (A,B) *In situ* hybridization (ISH) showing *tbx2b* expression in 72 hpf WT and *stx4* mutant larvae. *Stx4* mutants exhibit a loss of the midbrain-hindbrain transition. Mb: midbrain, Hb: hindbrain. Scale bar: 200 μM. (C,D) Brightfield images of 72 hpf WT and *stx4* mutant larvae otic vesicles. *Stx4* mutant have atrophic otic vesicles (outlined) with smaller otoliths. OV: otic vesicle. Scale bar: 200 μM. (E,F) Confocal images of 72 hpf WT and *stx4* mutant larvae labelled with IHC for Mhc (magenta) and *neurod:*EGFP (yellow). (E',F') *stx4* mutants with the *neurod:EGFP* transgene showing disorganized cerebellum (arrowhead) and fewer, less-organized retinal progenitor cells (asterisk). Scale bar: 100 μM. (G,H) Confocal max intensity projections (MIPs) of IHC on 72 WT and *stx4* mutant larvae labelled with cleaved-Caspase 3. *Stx4* mutants exhibit a significant amount of cell death, particularly in the brain and eye. Scale bar: 200 μM. (I-K) 72 hpf WT and *stx4* mutant larvae labelled with *o*-dianisidine, which labels hemoglobin in the erythrocytes (red). Asterisks indicate hemorrhaging from the craniopharyngeal or intersegmental vasculature observed in ~20% of mutant larvae (*n* = 9/44 zebrafish). Scale bar: 200 μM. (L,M) Confocal MIPs of 72 hpf WT or *stx4* mutant larvae carrying the *Tg(kdrl:EGFP*); *Tg(gata1:dsRed)* transgenes. (L',M') Single channel images showing *kdrl*:EGFP expression. Asterisk in K' indicates enlarged primordial mid/hindbrain channels and the agenesis of central arteries observed in *stx4* mutants. (L",M") Single channel images of *gata1*:dsRed. Arrowhead indicates hemorrhaging observed from central arteries in the forebrain of *stx4* mutant. Scale bar: 100 μM. Views in images are lateral with anterior up or to the left. (N) Survival curve of *stx4* mutant zebrafish. WT/*stx4*$^{+/-}$ zebrafish exhibit a 93.33% survival rate past 96 hpf, by contrast 30.77% of *stx4* mutants survive past 96 hpf and all die by 120 hpf. Data are represented as percent survival of *n* = 30 WT/*stx4*$^{+/-}$ and *n* = 26 *stx4*$^{-/-}$ mutant zebrafish, Log-rank (Mantel-Cox) test, ****$p < 0.0001$.

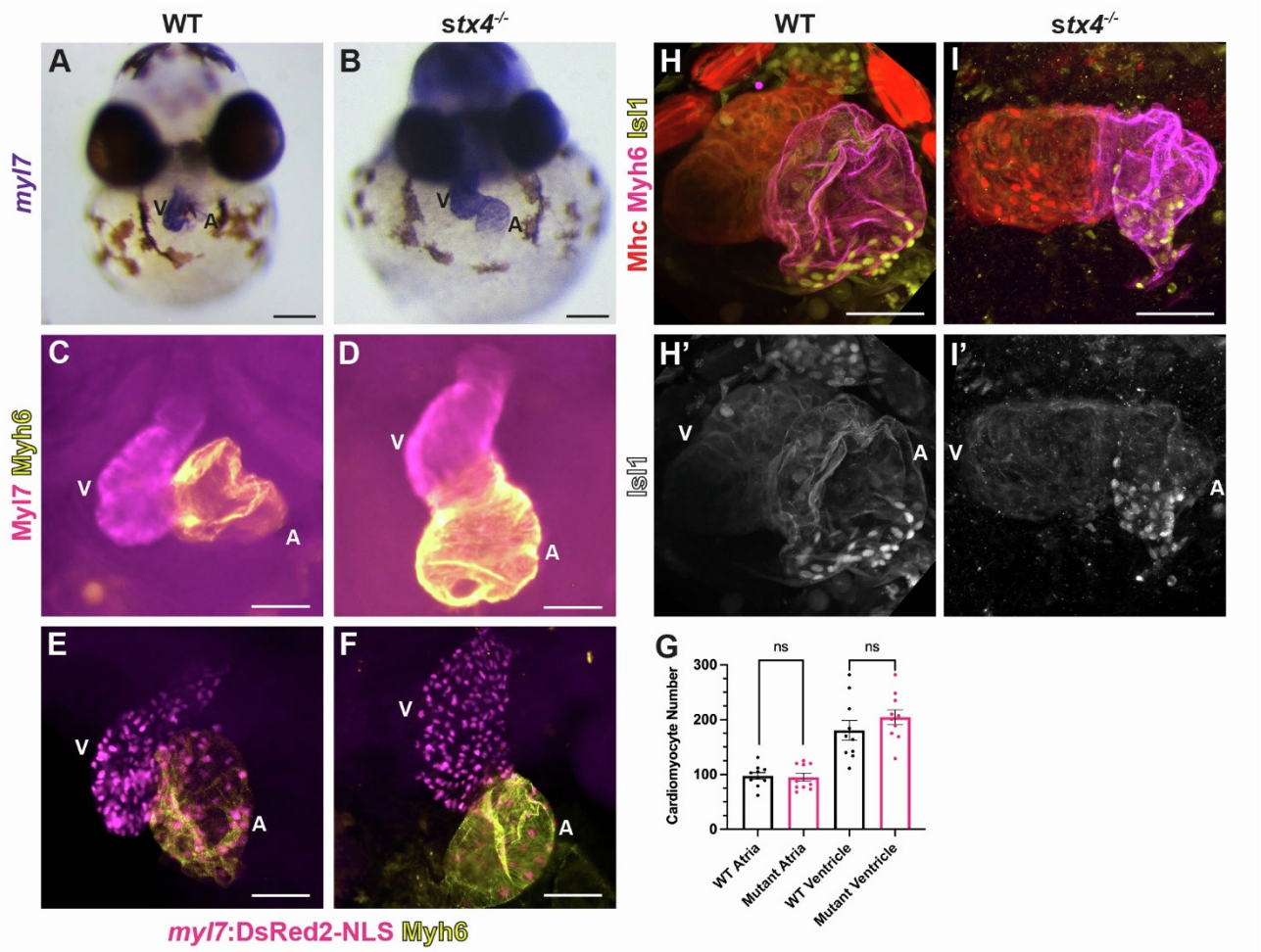


**Figure S6. Stx4 is dispensable for CM differentiation.** (A,B) Whole-mount ISH for *myl7* in 72 hpf WT and *stx4* mutant larvae. Frontal views. Scale bar: 100 μM. (C,D) IHC for Myh7 (ventricular CMs – magenta) and Myh6 (yellow) in hearts of 72 hpf WT and *stx4* mutant larvae. Scale bar: 50 μM. (E,F) IHC of representative hearts from 72 hpf WT and *stx4* mutant larvae carrying the *myl7:DsRed2-NLS* transgene and labeled for Myh6 (yellow) used for CM quantification. Scale bar: 50 μM. (G) Quantification of atrial and ventricular CMs hearts from 72 hpf WT and *stx4* mutant larvae. Data are represented as the mean ± SEM, *n* = 10 larvae/group, Student's t-test. (H,I) Confocal images of IHC for Mhc (magenta), Myh6 (red), and Isl1 (pacemaker CMs – yellow) in hearts of 72 hpf WT and *stx4* mutant larvae. (H',I') Single channel images of Isl1 at the venous pole. Scale bar: 50 μM. A: atrium; V: ventricle.

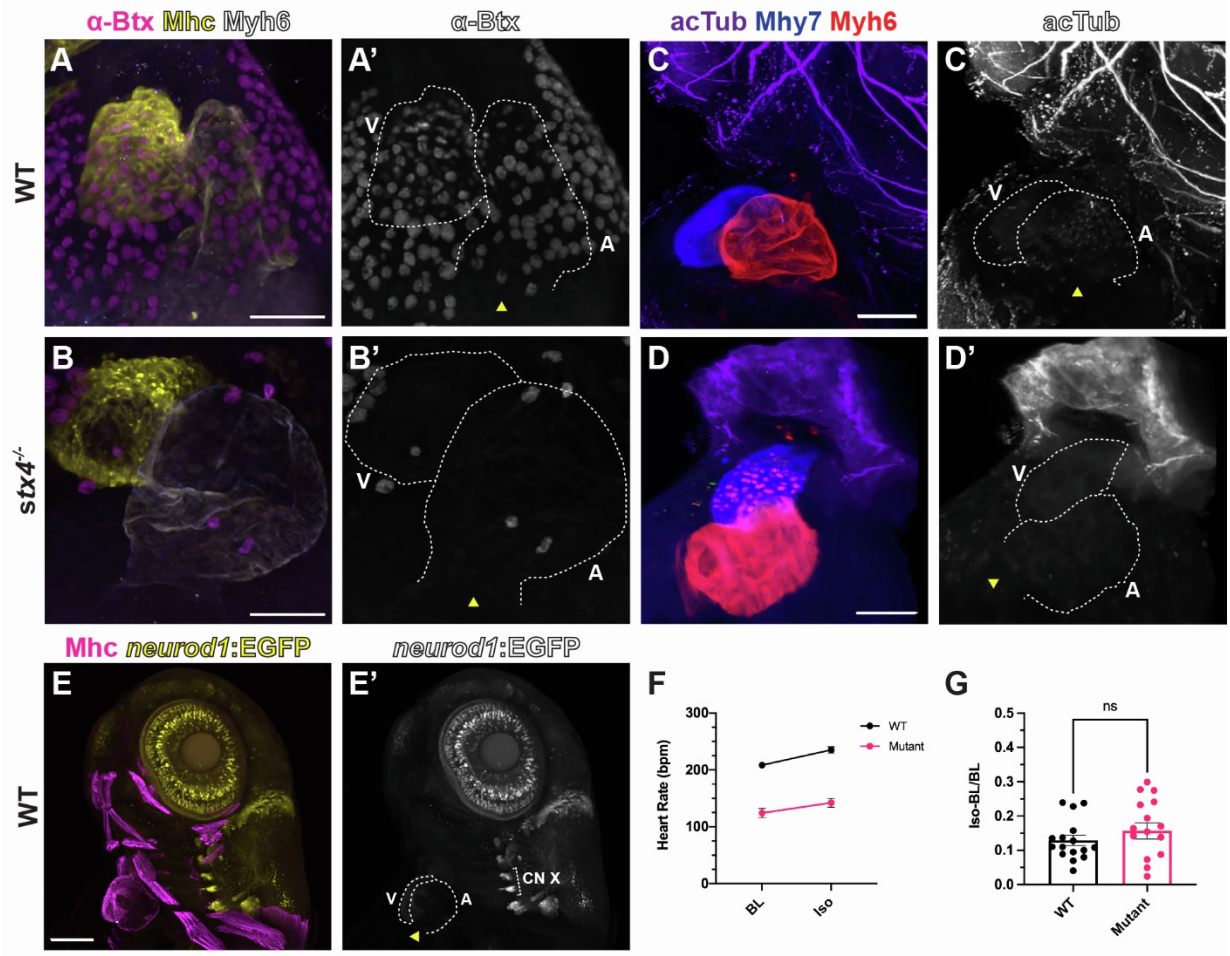


**Figure S7. Stx4 is dispensable for autonomic innervation or stimulation by 72 hpf.** (A,B) Confocal images of hearts from 72 hpf WT and *stx4* mutant larvae labelled for Mhc (white), Mhy6 (yellow), and conjugated α-Bungarotoxin (α-Btx), a nicotinic aceytocholine receptor neurotoxin (magenta). α-Btx labelling does not label cells at the venous pole of the hearts (yellow arrowheads) at 72 hpf, suggesting there is not parasympathetic input yet at this stage. Scale bar: 50 μM. (A',B') Single channel of α-Btx staining. White vesicles around the pericardial sac are hatching gland granules. (C,D) Confocal images of 72 hpf WT and *stx4* mutant larvae labelled for Myh6 (red), Myh7 (blue) and acetylated tubulin (acTub; purple). (C',D') Single channel image of acTub. AcTub, marking axonal projections was not detected at the venous poles of the heart (yellow arrowheads). Scale bar: 50 μM. (E) Confocal image of 72 hpf WT larvae carrying the *TgBAC(neurod:EGFP)* transgene, which labels cranial nerves including the vagus nerve, and labelled for Mhc (magenta). CN X: vagus nerve nuclei. (E') Single channel confocal image of *TgBAC(neurod:EGFP)*. No parasympathetic input from the vagus nerve is detected at 72 hpf at the base of the heart (arrowhead). Scale bar: 100 μM. (F,G) Heart rates determined from ventricular ROIs of 72 hpf WT and *stx4* mutant larvae captured by high-speed imaging and quantified as beats per minute (bpm) and the rate of change upon isoproterenol treatment relative to baseline (iso-BL/BL), imaged both before and after 30 minutes of treatment with 500 μM isoproterenol. Data are represented as the mean ± SEM, *n* = 16 larvae/group, Student's t-test. BL: baseline; iso: isoproterenol. A; atrium; V: ventricle.

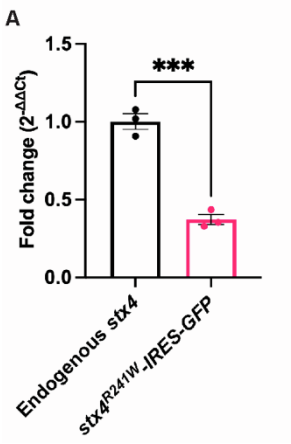


**Figure S8. Transgenic expression of *stx4*$^{R241W}$*-IRES-EGFP*.** RT-qPCR for *stx4*$^{R241W}$*-IRES-EGFP* expression from zebrafish hemizygous for the *actb2:stx4*$^{R241W}$*-IRES-EGFP* transgene relative to endogenous *stx4* in WT zebrafish at 72 hpf. Endogenous *stx4* was amplified using primers internal to *stx4* cDNA; transgenic *stx4*$^{R241W}$*-IRES-EGFP* was amplified using primers for *GFP*. *n* = 3 biological replicates of pooled (*n* = 25-30 embryos/pool) embryos assayed as technical triplicates. Student's t-test, ****$p < 0.0001$.

**Supplemental Tables**

**Table S1. Variants detected in Patient 1 by WES trio-analysis.**

| Gene Symbol | Chromosome (Cytoband) | Position[a] (Exon) | HGVS Nomenclature (Variant Type) | dbSNP RS ID | MIM | ACMG Criteria | Zygosity in Patient 1, Segregation (Known inheritance pattern of variant: disease manifestation) | Minor Allele Frequency[b] |
|---|---|---|---|---|---|---|---|---|
| Pathogenic/Likely Pathogenic Variants | | | | | | | | |
| *EXOSC8* | Chr13 (13q13.3) | 37583420 (Exon 11) | NM_181503.3: c.815G>C; p.Ser272Thr (SNV) | rs36027220 | 606019 | PS3 PP1 PP5 BP4 | Heterozygous, Maternal (AR: Pontocerebellar hypoplasia, type 1C [MIM: 616081]) | 0.00385 |
| *SLC26A4*[c] | Chr7 (7q22.3) | 107312690 (Exon 4) | NM_000441.2: c.412G>T; p.Val138Phe (SNV) | rs111033199 | 605646 | PS4 PM2 PM3 PP5 | Heterozygous, Maternal (AR: Deafness, autosomal recessive 4, with enlarged vestibular aqueduct [MIM: 600791]; AR: Pendred Syndrome [MIM: 274600]) | 0.000175 |
| *TREX1* | Chr3 (3p21.31) | 48508395 (Exon 1) | NM_016381.5: c.506G>A; p.Arg169His (SNV) | rs72556554 | 606609 | PS3 PM2 PM3 PP1 PP3 PP5 | Heterozygous, Paternal (AR/AD: Aicardi-Goutieres syndrome 1 [MIM: 225750]; AD: Chilblain lupus [MIM: 610448]; AD: Vasculopathy, retinal, with cerebral leukoencephalopathy and systemic manifestations [MIM: 192315]) | 0.000208 |
| | | | | | | | | |
| Variants of Uncertain Significance | | | | | | | | |
| *DSG2*[d] | Chr18 (18q12.1) | 29104553 (Exon 7) | NM_001943.5: c.828+5C>T (SNV) | rs373286117 | 125671 | PM2 BP4 | Heterozygous, Maternal | 0.00000806 |
| *TNXB*[e] | Chr6 (6p21.33) | 32052313 (Exon 8) | NM_019105.8: c.3322G>A; p.Val1108Met (SNV) | rs121912575 | 600985 | PM2 BP4 | Heterozygous, Paternal | 0.000827 |
| *STX4* | Chr16 (16p11.2) | 31050877 (Exon 9) | NM_004604.4: c.718C>T; p.Arg240Trp (SNV) | rs770931989 | 186591 | PM2 PP3 | Homozygous, Paternal/Maternal | 0.00000796 |

a. Sequence positions refer to human reference genome hg19.
b. MAFs were obtained from Varsome using gnomAD Exomes Version: 2.1.1 entries.
c. Targeted deletion and duplication analysis by comparative genomic hybridization was performed by the Genetics and Genomics Diagnostic Laboratory at Cincinnati Children's and was confirmed negative.
d. Other variants in this gene are associated with the following phenotypes: Arrhythmogenic right ventricular dysplasia 10 (autosomal dominant; MIM: 610193) and Cardiomyopathy, dilated, 1BB (MIM: 612877); however, this variant is not predicted to affect exon splicing.
e. Other SNVs in TNXB are associated with Ehlers-Danlos syndrome, classic-like, 1 (autosomal recessive; MIM: 606408) and Vesicoureteral reflux 8 (autosomal dominant; MIM: 615963), which is not concordant with Patient 1's phenotype. A clinical testing submission of this variant were reported as "Likely Benign" on Varsome and ClinVar.

**Table S2. Variants detected in Patient 2 by WES trio-analysis.**

| Gene Symbol | Chromosome (Cytoband) | Position[a] (Intron/ Exon) | HGVS Nomenclature (Variant Type) | dbSNP RS ID | MIM | ACMG Criteria | Zygosity in Patient 2, Segregation (Known inheritance pattern of variant: disease manifestation) | Minor Allele Frequency[b] |
|---|---|---|---|---|---|---|---|---|
| Pathogenic/Likely Pathogenic Variants | | | | | | | | |
| *EIF3F*[c] | Chr11 (11p15.4) | 8016013 (Exon 5) | NM_003754.2: c.694T>G; p.Phe232Val (SNV) | rs141976414 | 603914 | PM2 PP3 PP5 | Homozygous, Paternal/Maternal (AR: Intellectual Developmental Disorder, 67 [MIM: 618295]) | 0.000701 |
| *XDH*[e] | Chr2 (2p23.1) | 31560605 (Exon 35) | NM_000379.3: c.3853C>T; p.Gln1285* (SNV) | rs761545629 | 607633 | PVS1 PM2 PP3 | Compound heterozygous, Maternal | 0.00000398 |
| | | | | | | | | |
| Variants of Uncertain Significance | | | | | | | | |
| *STX4* | Chr16 (16p11.2) | 31045392 (Exon 2) | NM_004604.4: c.89_90delGC; p.Gly30Aspfs*28 (DEL) | rs1301001687 | 186591 | PM2 | Compound heterozygous, Paternal | 0.0000000000301[d] |
| *STX4* | Chr16 (16p11.2) | 31045650 (Intron 3) | NM_004604.4: c.232+4A>C (SNV) | rs922762463 | 186591 | PM2 PP3 | Compound heterozygous, Maternal | 0.00000399 |
| *XDH*[f] | Chr2 (2p23.1) | 31595130 (Exon 17) | NM_000379.3: c.1820G>A; p.Arg607Gln (SNV) | rs45442092 | 607633 | BP6 | Compound heterozygous, Paternal | 0.00203 |
| *COL22A1* | Chr8 (8q24.23) | 139772485 (Intron 18) | NM_152888.3: c.1902+1G>A (SNV) | rs372694589 | 610026 | PM2 PP3 | Compound heterozygous, Paternal | 0.0000723 |
| *COL22A1* | Chr8 (8q24.23) | 139629176 (Exon 53) | NM_152888.3: c.3851C>T; p.Ser1284Phe (SNV) | rs200631977 | 610026 | PM2 BP4 | Compound heterozygous, Maternal | 0.0000318[g] |
| *DNAH2*[h] | Chr17 (17p13.1) | 7674168 (Exon 27) | NM_020877.4: c.4279G>C; p.Asp1427His (SNV) | | 603333 | PM2 PP3 BP1 | Compound heterozygous, Paternal | 0.00000000000192 |
| *DYSF*[i] | Chr2 (2p13.2) | 71797041 (Exon 27) | NM_003494.4: c.2902A>T; | rs144636654 | 603009 | PM2 BP4 | Compound heterozygous, Paternal | 0.00140 |

| | | | | | | | | |
|---|---|---|---|---|---|---|---|---|
| | | | p.Met968Leu (SNV) | | | | (AR: Miyoshi muscular dystrophy 1 [MIM: 254130] ; AR: Muscular dystrophy, limb-girdle, 2 [MIM: 253601]) | |
| *TNK2*[j] | Chr3 (3q29) | 195594879 (Exon 13) | NM_001010938.2: c.2479C>A; p.Pro827Thr (SNV) | | 606994 | PM2 PP3 | Compound heterozygous, Maternal | 0.00000000000155 |
| *TNS4*[k] | Chr13 (17q21.2) | 38643441 (Exon 4) | NM_032865.6: c.1135G>C; p.Gly379Arg (SNV) | | 608385 | PM2 PP3 | Compound heterozygous, Maternal | 0.00000000000200 |
| *OPRK1* | Chr8 (8q11.23) | 54142245 (Exon 3) | NM_000912.5: c.755G>A; p.Arg252His (SNV) | rs200672427 | 165196 | PM2 PP3 | De novo | 0.00000398 |
| *CACNG8* | Chr19 (19q13.42) | 54485817 (Exon 4) | NM_031895.6: c.992_994del; p.Gly331del (DEL) | rs769981108 | 606900 | PM2 BP4 | Mosaic, Maternal | 0.0000391 |

a. Sequence positions refer to human reference genome hg19.
b. MAFs were obtained from Varsome using gnomAD Exomes Version: 2.1.1 entries.
c. Previous associations were not concordant with Patient 2's phenotype;[1,2] however, this variant was noted as an additional finding upon postnatal re-evaluation of the WES trio-analysis.
d. gnomAD MAF was not available. MAF computed from in-house global allele frequency.
e. Other variants in this gene are associated with Xanthinuria, type I (autosomal recessive; MIM: 278300) and Xanthinuria, type II (autosomal recessive; MIM: 603592), which are not concordant with patient 2's phenotype or zygosity.
f. This variant was associated with lowered activity in xanthine dehydrogenase in cell culture;[3] however, two clinical testing submissions of this variant were reported as "Likely Benign" on Varsome and ClinVar.
g. gnomAD MAF was not available. MAF computed from in-house global allele frequency.
h. An additional heterozygous maternal SNV was synonymous. gnomAD MAF was not available. MAF computed from in-house global allele frequency. Other variants in this gene are associated with Spermatogenic failure 45 (autosomal recessive; MIM: 619094).
i. Conflicting interpretations of pathogenicity are reported for this variant in association with the listed conditions. Two additional heterozygous maternal alleles (NM_003494.4:c.3065G>A; p.Arg1022Gln [RS ID: rs34211915] and NM_003494.4:c.3992G>T; p.Arg1331Leu [RS ID: rs61742872]) were indicated as "Benign" by *in silico* prediction methods.

j. An additional heterozygous paternal SNV was filtered out due to quality. gnomAD MAF was not available. MAF computed from in-house global allele frequency.

k. An additional heterozygous paternal SNV was filtered out due high MAF and indication as "Likely Benign". gnomAD MAF was not available. MAF computed from in-house global allele frequency.

**Table S3. List of primer sequences used.**

| Name | Sequence |
|---|---|
| Patient sequencing primers: | |
| *R240W_F* | *5'*- CTTACCTCCCTGAACCACCC-*3'* |
| *R240W_R* | *5'*- CTCACCTTCCTCGCCTTCTT-*3'* |
| | |
| *In situ* primers: | |
| *stx4-probe-F1* | *5'*- TCGCCCCACACTGATCTCTA-*3'* |
| *stx4-probe-R1* | *5'*- GTCCACCATCTCACCCTGTG-*3'* |
| | |
| gRNAs: | |
| *stx4-t2* gRNA | *5'*-GCTAGGAGTTGCACTTCCAG-*3'* |
| | |
| Zebrafish sequencing primers: | |
| *stx4-t2-F1* | *5'*- GAGATTCGAGAGGGACTTGAAA-*3'* |
| *stx4-t2-R1* | *5'*- CCTTTTTCATACCTGTGCTCAA-*3'* |
| | |
| Gateway cloning: | |
| *GFP-seq-F2* | *5'*- AGAAGAACGGCATCAAGGTG-*3'* |
| *M13 Forward (-20)* | *5'*- GTAAAACGACGGCCAGT-*3'* |
| *M13 Reverse* | *5'*-CAGGAAACAGCTATGAC-*3'* |
| *stx4-attB1-F1* | *5'*-GGGGACAAGTTTGTACAAAAAAGCAGGCTTTCAC CATGCGGGACCGGACCAAAGAACTG-*3'* |
| *stx4-attB2-R1* | *5'*-GGGGACCACTTTGTACAAGAAAGCTGGGTTTCAA GAGAAACTGATAGCCAGGCA-*3'* |
| *stx4-RT-F2* | *5'*-GTTCAGGAGATTCGAGAGGGACTTG-*3'* |
| *stx4-RT-R3* | *5'*-ACACCATGCTGAGTTCTCCTC-*3'* |
| | |
| QuikChange II primers: | |
| *stx4R241W-QC-F* | *5*'-GCACAGGGTGAGATGGTGGACTGGATTGAGTCG AACATTA-*3'* |
| *stx4R241W-QC-R* | *5*'-GGGACATTTTAATGTTCGACTCAATCCAGTCCAC CATCTC-*3'* |
| | |
| RT-qPCR primers: | |
| *stx4-RT-F4* | *5'*-CAGAGACCGAAATGTGGAG-*3'* |
| *stx4-RT-R4* | *5'*-ATCGTGTCGTGACTCAATC-*3'* |
| *gfp forward* | *5'*-CCAGATCCGCCACAACATCG-*3'* |
| *gfp reverse* | *5'*-GTCCATGCCGAGAGTGATCC-*3'* |
| *actb2 forward* | *5'*-TACAGCTTCACCACCACAGC-*3'* |
| *actb2 reverse* | *5'*-AGGAAGGAAGGCTGGAAGAG-*3'* |

**Table S4. List of antibodies used.**

| Name | Host | Clonality; Isotype | Manufacturer | Catalogue number | Dilution |
|---|---|---|---|---|---|
| Primary antibodies | | | | | |
| anti-acetylated Tubulin | Mouse | Monoclonal; IgG2b | Sigma Aldrich | T7451 | 1:250 |
| anti-cleaved Caspase 3 | Rabbit | Polyclonal | BD Biosciences | 559565 | 1:250 |
| anti-Alcama | Mouse | Monoclonal; IgG1 | University of Iowa Developmental Studies Hybridoma Bank (DSHB) | zn-8-s | 1:10 |
| anti-DsRed2 | Rabbit | Polyclonal | Clontech | 632496 | 1:1000 |
| anti-Isl1 | Rabbit | Polyclonal | Genetex | GTX128201 | 1:00 |
| anti-Sarcomeric Myosin Heavy Chain (Mhc) | Mouse | Monoclonal; IgG2b | DSHB | MF20 | 1:10 |
| anti-Atrial Myosin Heavy Chain (Myh6) | Mouse | Monoclonal; IgG1 | DSHB | S46 | 1:10 |
| anti-zebrafish Ventricular Myosin Heavy Chain (Myh7) | Rabbit | Polyclonal | YenZym | | 1:200 |
| anti-Syntaxin 4 | Rabbit | Polyclonal | Sigma Millipore | AB5330 | 1:400 |
| anti-Vamp2 | Rabbit | Polyclonal | Genetex | GTX132130 | 1:200 |
| | | | | | |
| Secondary antibodies | | | | | |
| anti-mouse IgG2b Alexa Fluor®-647 | Goat | Polyclonal | Southern Biotech | 1091-31 | 1:250 |
| anti-rabbit IgG(H+L) Alexa Fluor®-647 | Goat | Polyclonal | Southern Biotech | 4050-31 | 1:250 |
| anti-rabbit IgG (H+L) Cascade blue | Goat | Polyclonal | Life Technologies | C-2764 | 1:00 |
| anti-Mouse IgG1 DyLight™-405 | Goat | Polyclonal | Bio Legend | 409109 | 1:00 |
| anti-mouse IgG1-FITC | Goat | Polyclonal | Southern Biotech | 107002 | 1:100 |
| anti-rabbit IgG-FITC | Goat | Polyclonal | Southern Biotech | 405002 | 1:100 |
| anti-mouse IgG1-TRITC | Goat | Polyclonal | Southern Biotech | 107003 | 1:100 |
| anti-mouse IgG2b-TRITC | Goat | Polyclonal | Southern Biotech | 109003 | 1:100 |
| anti-rabbit IgG-TRITC | Goat | Polyclonal | Southern Biotech | 405003 | 1:100 |

**Supplemental References:**

1. Martin, H.C., Jones, W.D., McIntyre, R., Sanchez-Andrade, G., Sanderson, M., Stephenson, J.D., Jones, C.P., Handsaker, J., Gallone, G., Bruntraeger, M., et al. (2018). Quantifying the contribution of recessive coding variation to developmental disorders. Science (80-. ). *362*, 1161–1164.

2. Csibi, A., Cornille, K., Leibovitch, M.P., Poupon, A., Tintignac, L.A., Sanchez, A.M.J., and Leibovitch, S.A. (2010). The translation regulatory subunit eiF3f controls the kinase-dependent mTOR signaling required for muscle differentiation and hypertrophy in mouse. PLoS One *5*,.

3. Kudo, M., Moteki, T., Sasaki, T., Konno, Y., Ujiie, S., Onose, A., Mizugaki, M., Ishikawa, M., and Hiratsuka, M. (2008). Functional characterization of human xanthine oxidase allelic variants. Pharmacogenet. Genomics *18*, 243–251.